High-pressure Synthesis and Characterization of the Fluoride Borate $Tm_5(BO_3)_2F_9$

Almut Haberer[a], Michael Enders[a], Reinhard Kaindl[b], and Hubert Huppertz[a]

[a] Institut für Allgemeine, Anorganische und Theoretische Chemie, Leopold-Franzens-Universität Innsbruck, Innrain 52a, 6020 Innsbruck, Austria
[b] Institut für Mineralogie und Petrographie, Leopold-Franzens-Universität Innsbruck, Innrain 52, 6020 Innsbruck, Austria

Reprint requests to H. Huppertz. E-mail: Hubert.Huppertz@uibk.ac.at

Z. Naturforsch. **2010**, *65b,* 1213 – 1218; received June 17, 2010

The rare earth fluoride borate $Tm_5(BO_3)_2F_9$ was synthesized from Tm_2O_3, B_2O_3, and TmF_3 under high-pressure/high-temperature conditions of 5 GPa and 900 °C in a Walker-type multianvil apparatus. The single-crystal structure determination revealed that $Tm_5(BO_3)_2F_9$ is isotypic to the compounds $RE_5(BO_3)_2F_9$ (RE = Er, Yb). $Tm_5(BO_3)_2F_9$ crystallizes in the space group $C2/c$ ($Z = 4$) with the parameters $a = 2030.9(4)$, $b = 606.2(2)$, $c = 822.6(2)$ pm, $\beta = 100.5(1)°$, $V = 995.7(3)$ Å^3, $R_1 = 0.0341$, and $wR_2 = 0.0724$ (all data). The structure is composed of isolated BO_3 groups, ninefold coordinated thulium cations, and fluoride anions. Infrared and Raman spectroscopic data of $Tm_5(BO_3)_2F_9$ are compared to the data of $RE_5(BO_3)_2F_9$ (RE = Er, Yb).

Key words: Rare Earth, Fluoride, Borate, High Pressure, Crystal Structure

Introduction

In the chemistry of rare-earth fluoride borates, the first known compounds $RE_3(BO_3)_2F_3$ (RE = Sm, Eu, Gd) [1, 2] and $Gd_2(BO_3)F_3$ [3] were obtained through the heating of stoichiometric mixtures of RE_2O_3, B_2O_3, and REF_3 under ambient-pressure conditions. In the last two years, the implementation of high-pressure/high-temperature techniques have given access to four new structure types with the compositions $RE_5(BO_3)_2F_9$ (RE = Er, Yb) [4, 5], $La_4B_4O_{11}F_2$ [6], $Gd_4B_4O_{11}F_2$ [7], and $Pr_4B_3O_{10}F$ [8]. Recently, the first divalent rare-earth fluoride borate $Eu_5(BO_3)_3F$ [9] was synthesized by Kazmierczak *et al.* under ambient-pressure conditions. The successful syntheses of the phases $RE_5(BO_3)_2F_9$ (RE = Er, Yb) [4, 5] indicated that most likely this structure type may also exist with the rare-earth cation Tm^{3+}. While $Er_5(BO_3)_2F_9$ and $Yb_5(BO_3)_2F_9$ were synthesized at 3 GPa and 7.5 GPa, respectively, now, the isotypic thulium fluoride borate $Tm_5(BO_3)_2F_9$ could be synthesized successfully at a pressure of 5 GPa. In this paper, we report the high-pressure synthesis of $Tm_5(BO_3)_2F_9$, including a comparison with the isotypic compounds $RE_5(BO_3)_2F_9$ (RE = Er, Yb) with respect to structural and spectroscopic data.

Experimental Section

Synthesis

The synthesis of $Tm_5(BO_3)_2F_9$ was achieved under high-pressure/high-temperature conditions of 5 GPa and 900 °C. A stoichiometric mixture of B_2O_3 (Strem Chemicals, 99.9+ %), Tm_2O_3 (Strem Chemicals, 99.9+ %), and TmF_3 (Alfa Aesar GmbH & Co KG, 99+ %) was pestled in a glove box and filled into a boron nitride crucible (Henze BNP GmbH, HeBoSint® S100, Kempten, Germany). The latter was positioned into an 18/11 assembly, which was compressed by eight tungsten carbide cubes (TSM-20, Ceratizit, Reutte, Austria) in a Walker-type multianvil device and a 1000 ton press (both devices from the company Voggenreiter, Mainleus, Germany). A detailed description of the assembly can be found in the references [10 – 14].

The 18/11 assembly was compressed to 5 GPa in 135 min, heated to 900 °C (cylindrical graphite furnace) within 15 min, kept at this temperature for 20 min, and cooled down to 700 °C during another 20 min. After cooling to r. t. by radiation heat loss, the decompression of the assembly lasted 7 h. The recovered octahedral pressure medium (MgO, Ceramic Substrates & Components Ltd., Newport, Isle of Wight, UK) was broken apart and the surrounding boron nitride and graphite were separated from the sample. This procedure yielded colorless air- and water-resistant crystals of the compound $Tm_5(BO_3)_2F_9$.

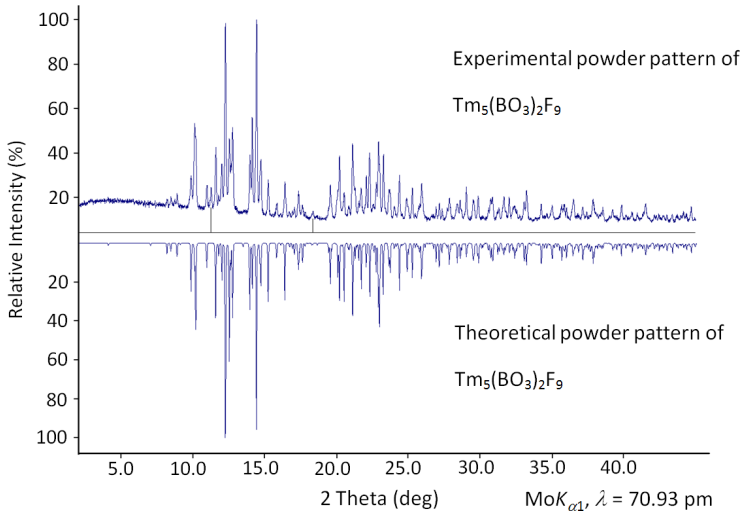

Fig. 1 (color online). Top: experimental powder pattern of $Tm_5(BO_3)_2F_9$; reflections of an unknown phase are indicated with lines. Bottom: theoretical powder pattern of $Tm_5(BO_3)_2F_9$ based on single-crystal diffraction data.

Table 1. Crystal data and structure refinement of $Tm_5(BO_3)_2F_9$ (standard deviations in parentheses).

Empirical formula	$Tm_5(BO_3)_2F_9$
Molar mass, g mol^{-1}	1133.27
Crystal system	monoclinic
Space group	*C*2/*c*
Powder diffractometer	Stoe STADI P
Radiation	Mo$K_{\alpha1}$ (λ = 70.93 pm)
Powder data	
a, pm	2030.1(8)
b, pm	605.8(4)
c, pm	822.7(5)
β, deg	100.6(1)
V, Å^3	994.7(7)
Single-crystal diffractometer	Nonius Kappa CCD
Radiation	MoK_α (λ = 71.073 pm)
Crystal size, mm^3	0.04 × 0.04 × 0.06
Single-crystal data	
a, pm	2030.9(4)
b, pm	606.2(2)
c, pm	822.6(2)
β, deg	100.5(1)
V, Å^3	995.7(3)
Formula units per cell *Z*	4
Calculated density, g cm^{-3}	7.56
Temperature, K	293(2)
Absorption coefficient, mm^{-1}	44.3
F(000), e	1936
θ range, deg	2.0 – 32.5
Range in *hkl*	±30, ±9, ±12
Total no. of reflections	6212
Independent reflections / R_{int} / R_σ	1809 / 0.0583 / 0.0422
Reflections with $I \geq 2\sigma(I)$	1643
Data / ref. parameters	1809 / 102
Absorption correction	multi-scan
Final *R*1 / *wR*2 [$I \geq 2\sigma(I)$]	0.0296 / 0.0702
*R*1 / *wR*2 (all data)	0.0341 / 0.0724
Goodness-of-fit on F^2	1.058
Largest diff. peak and hole, e Å^{-3}	3.7 / −3.2

Table 2. Atomic coordinates and isotropic equivalent displacement parameters U_{eq} (Å^2) for $Tm_5(BO_3)_2F_9$ (space group: *C*2/*c*) (standard deviations in parentheses). U_{eq} is defined as one third of the trace of the orthogonalized U_{ij} tensor.

Atom	W.-position	*x*	*y*	*z*	U_{eq}
Tm1	8*f*	0.30677(2)	0.11941(4)	0.18042(3)	0.00654(9)
Tm2	8*f*	0.39044(2)	0.38928(4)	0.59287(3)	0.0083(2)
Tm3	4*e*	1/2	0.11053(6)	1/4	0.0082(2)
B1	8*f*	0.3885(5)	0.904(2)	0.437(2)	0.018(3)
O1	8*f*	0.4094(2)	0.7583(7)	0.5648(5)	0.0077(8)
O2	8*f*	0.3385(2)	0.0698(9)	0.4625(6)	0.0123(9)
O3	8*f*	0.4075(2)	0.1050(7)	0.7813(6)	0.0094(9)
F1	8*f*	0.2891(3)	0.4227(7)	0.0198(5)	0.0105(7)
F2	8*f*	0.3683(2)	0.5758(7)	0.8134(5)	0.0119(7)
F3	4*e*	1/2	0.4879(9)	1/4	0.014(2)
F4	8*f*	0.2740(2)	0.7807(7)	0.2167(5)	0.0135(8)
F5	8*f*	0.4688(2)	0.1851(8)	0.5136(6)	0.0209(9)

Crystal structure analysis

$Tm_5(BO_3)_2F_9$ was identified by X-ray powder diffraction on a flat sample of the reaction product, using a Stoe Stadi P powder diffractometer with Mo$K_{\alpha1}$ radiation (transmission geometry, Ge monochromator, λ = 70.93 pm). Fig. 1 shows the powder pattern displaying reflections of $Tm_5(BO_3)_2F_9$ as well as a still unknown side product (marked with lines in Fig. 1). The experimental powder pattern (top) is in good agreement with the theoretical pattern (bottom), simulated from the single-crystal data. Indexing the reflections of the thulium fluoride borate, we derived the parameters *a* = 2030.1(8), *b* = 605.8(4), *c* = 822.7(5) pm, β = 100.6(1)° and a volume of 994.7(7) Å^3. This validated the lattice parameters received from the single-crystal X-ray diffraction data (Table 1). Intensity data of a single crystal of $Tm_5(BO_3)_2F_9$ were gathered at r. t. by use of a Kappa CCD diffractometer (Bruker AXS/Nonius, Karlsruhe), equipped with a Miracol fiber optics collimator and a Nonius FR590

Table 3. Anisotropic displacement parameters U_{ij} (Å^2) for $Tm_5(BO_3)_2F_9$ (space group *C*2/*c*).

Atom	U_{11}	U_{22}	U_{33}	U_{12}	U_{13}	U_{23}
Tm1	0.0080(2)	0.0047(2)	0.0069(2)	−0.00038(8)	0.0013(2)	0.00022(8)
Tm2	0.0148(2)	0.0045(2)	0.0055(2)	−0.00022(8)	0.0015(2)	0.00286(8)
Tm3	0.0057(2)	0.0091(2)	0.0097(2)	0	0.0012(2)	0
B1	0.023(4)	0.012(3)	0.019(4)	−0.001(3)	0.006(3)	−0.003(3)
O1	0.011(2)	0.005(2)	0.008(2)	0.000(2)	0.002(2)	−0.001(2)
O2	0.009(2)	0.020(2)	0.007(2)	0.005(2)	−0.002(2)	−0.007(3)
O3	0.011(2)	0.010(2)	0.007(2)	0.000(2)	0.001(2)	0.000(2)
F1	0.006(2)	0.013(2)	0.012(3)	0.001(2)	0.002(2)	−0.001(2)
F2	0.021(2)	0.007(2)	0.008(2)	0.001(2)	0.003(2)	0.007(3)
F3	0.014(3)	0.010(3)	0.017(3)	0	0.000(2)	0
F4	0.015(2)	0.012(3)	0.013(2)	0.001(2)	0.002(2)	−0.006(2)
F5	0.016(2)	0.022(2)	0.026(2)	−0.009(3)	0.007(2)	−0.003(2)

Table 4. Interatomic distances (pm) in $Tm_5(BO_3)_2F_9$ (space group: *C*2/*c*), calculated with the single-crystal lattice parameters (standard deviations in parentheses).

Tm1–O3	247.0(5)	Tm2–O3	230.2(5)	Tm3–O3	234.1(5)
Tm1–O1	255.4(5)	Tm2–O1	228.9(5)		2 ×
Tm1–O2a	231.2(5)	Tm2–O2	236.7(6)	Tm3–O1	230.6(5)
Tm1–O2b	231.6(5)	Tm2–F1	233.4(4)		2 ×
Tm1–F1a	225.5(4)	Tm2–F3	247.6(3)	Tm3–F3	228.7(6)
Tm1–F1b	232.3(4)	Tm2–F5	220.7(5)	Tm3–F5a	241.0(5)
Tm1–F4a	219.5(4)	Tm2–F4	292.7(4)		2 ×
Tm1–F4b	220.7(4)	Tm2–F2a	225.1(4)	Tm3–F5b	263.5(5)
Tm1–F2	238.2(4)	Tm2–F2b	227.1(4)		2 ×
	∅ = 233.5		∅ = 238.0		∅ = 240.8
B1–O3	140.6(11)				
B1–O1	137.9(10)				
B1–O2	146.9(10)				
	∅ = 141.8				
F1–Tm1a	225.5(4)	F2–Tm1	238.2(4)	F3–Tm2	247.5(3)
F1–Tm1b	232.3(4)	F2–Tm2a	225.1(4)		2 ×
F1–Tm2	233.4(4)	F2–Tm2b	227.1(4)	F3–Tm3	228.7(6)
	∅ = 230.4		∅ = 230.1		∅ = 241.2
F4–Tm1a	219.5(4)	F5–Tm2	220.7(5)		
F4–Tm1b	220.7(4)	F5–Tm3a	241.0(5)		
F4–Tm2	292.7(4)	F5–Tm3b	263.5(5)		
	∅ = 244.3		∅ = 241.7		

Table 5. Interatomic angles (deg) in $Tm_5(BO_3)_2F_9$ (space group: *C*2/*c*), calculated with the single-crystal lattice parameters (standard deviations in parentheses).

O1–B1–O3	124.8(7)	Tm1a–F1–Tm1b	110.4(2)
O1–B1–O2	117.1(7)	Tm1a–F1–Tm2	102.0(2)
O3–B1–O2	117.9(7)	Tm1b–F1–Tm2	145.2(3)
	∅ = 119.9		∅ = 119.2
Tm3–F3–Tm2a	107.5(2)	Tm2–F5–Tm3a	133.9(2)
Tm3–F3–Tm2b	107.5(2)	Tm2–F5–Tm3b	104.6(3)
Tm2a–F3–Tm2b	145.0(3)	Tm3a–F5–Tm3b	117.9(3)
	∅ = 120.0		∅ = 118.8
Tm1a–F4–Tm1b	137.0(2)	Tm2a–F2–Tm2b	146.1(3)
Tm1a–F4–Tm2	89.8(3)	Tm2a–F2–Tm1	100.6(2)
Tm1b–F4–Tm2	132.9(3)	Tm2–F2–Tm1	112.5(2)
	∅ = 119.9		∅ = 119.7

generator (graphite-monochromatized MoK_α radiation, λ = 71.073 pm). An absorption correction, based on multi-scans, was performed with SCALEPACK [15]. All significant details of the data collection and analyses are listed in Table 1. For the structure refinement, the positional parameters of the isotypic compound $Er_5(BO_3)_2F_9$ were used as starting values [4]. The parameter refinement (full-matrix least-squares against F^2) was achieved by using SHELXL-97 [16, 17]. All atoms were refined with anisotropic atomic displacement parameters. The final difference Fourier syntheses did not reveal any significant residual peaks in all refinements. The positional parameters of the atom refinements, anisotropic displacement parameters, interatomic distances, and interatomic angles are listed in the Tables 2 – 5.

Table 6. Comparison of the lattice parameters (pm, deg) and cell volumes V (Å^3) of $RE_5(BO_3)_2F_9$ (*RE* = Er, Tm, Yb) (standard deviations in parentheses).

Compound	*a*	*b*	*c*	*β*	*V*
$Er_5(BO_3)_2F_9$	2031.2(4)	609.5(2)	824.6(2)	100.3(1)	1004.4(3)
$Tm_5(BO_3)_2F_9$	2030.9(4)	606.2(2)	822.6(2)	100.5(1)	995.7(3)
$Yb_5(BO_3)_2F_9$	2028.2(4)	602.5(2)	820.4(2)	100.6(1)	985.3(3)

Further details of the crystal structure investigation may be obtained from the Fachinformationzentrum Karlsruhe, 76344 Eggenstein-Leopoldshafen, Germany (fax: +49-7247-808-666; e-mail: crysdata@fiz-karlsruhe.de, http://www.fiz-informationsdienste.de/en/DB/icsd/depot_anforderung.html) on quoting the deposition number CSD-421889.

Results and Discussion

Crystal structure of $Tm_5(BO_3)_2F_9$

The structure of $Tm_5(BO_3)_2F_9$ consists of isolated BO_3 groups, ninefold coordinated thulium cations, and fluoride anions (Fig. 2). For a detailed depiction of the structure, the reader is referred to the description of the isotypic compound $Yb_5(BO_3)_2F_9$ [5]. In this paper, a comparison of the three isotypic compounds $RE_5(BO_3)_2F_9$ (*RE* = Er, Tm, Yb) is given.

Table 6 shows the values of the lattice parameters of $Er_5(BO_3)_2F_9$ [4], $Tm_5(BO_3)_2F_9$, and $Yb_5(BO_3)_2F_9$ [5]. The differences correspond to the decreasing

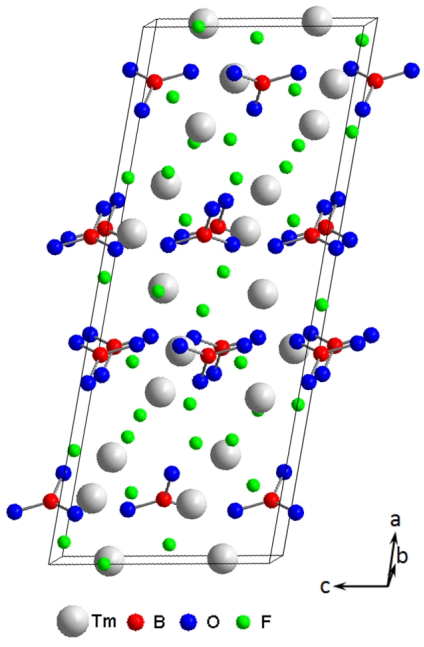

Fig. 2 (color online). Crystal structure of $Tm_5(BO_3)_2F_9$, showing isolated BO_3 groups.

ionic radii (lanthanoide contraction) of the ninefold coordinated rare-earth cations Er^{3+} (ionic radius = 120 pm [18]), compared to Tm^{3+} (119 pm [18]), and Yb^{3+} (118 pm [18]). Because the size differences are not too large, the bond lengths and angles in $Tm_5(BO_3)_2F_9$ are comparable to the values found in $Er_5(BO_3)_2F_9$ and $Yb_5(BO_3)_2F_9$. The Tm–O/F distances range from 219.5(4) to 292.7(4) pm, which fits well to the values of 220.9(3) – 288.8(4) pm for Er–O/F in $Er_5(BO_3)_2F_9$ and 218.6(4) – 294.2(5) pm for Yb–O/F in $Yb_5(BO_3)_2F_9$. The mean Tm–F distance is 237.5 pm, which is between the mean bond lengths of 238.1 and 236.9 pm in $Er_5(BO_3)_2F_9$ and $Yb_5(BO_3)_2F_9$, respectively. The B–O distances in $Tm_5(BO_3)_2F_9$ are in the range from 137.9(10) pm to 146.9(10) pm (Table 4), which is the same as found in $Er_5(BO_3)_2F_9$ (136.4(7) – 146.1(8) pm) and $Yb_5(BO_3)_2F_9$ (138.7(10) – 148.0(12) pm).

We also calculated the charge distribution of the atoms in $Tm_5(BO_3)_2F_9$ *via* bond valence sums ($\sum$V) using VALIST (Bond Valence Calculation and Listing) [19 – 21] and *via* the CHARDI (*char*ge *di*stribution in solids) concept ($\sum$Q) [22], verifying the formal valence states in the fluoride borate. Table 7 shows the formal ionic charges, received from the calculations, which correspond to the expected values.

Table 7. Charge distribution in $Tm_5(BO_3)_2F_9$, calculated with VALIST (ΣV) [19] and the CHARDI concept (ΣQ) [22].

	Tm1	Tm2	Tm3	B1
ΣV	2.95	2.79	2.63	2.66
ΣQ	3.04	2.94	3.05	3.00
	O1	O2	O3	F1
ΣV	−2.01	−1.99	−2.03	−0.87
ΣQ	−2.14	−1.81	−2.01	−1.09
	F2	F3	F4	F5
ΣV	−0.88	−0.66	−0.81	−0.71
ΣQ	−1.13	−0.88	−0.93	−0.95

Additionally, we calculated the MAPLE value (*Ma*delung *P*art of *L*attice *E*nergy according to Hoppe [23 – 25]) of $Tm_5(BO_3)_2F_9$, and checked it against the sum of the MAPLE values received from the binary compounds Tm_2O_3 [26], B_2O_3-I [27], and TmF_3 [28]. We obtained a value of 53842 kJ mol^{-1} for $Tm_5(BO_3)_2F_9$, compared to 53544 kJ mol^{-1} (deviation: 0.6 %), starting from the binary components [1 × Tm_2O_3 (15484 kJ mol^{-1}) + 1 × B_2O_3-I (20669 kJ mol^{-1}) + 3 × TmF_3 (5797 kJ mol^{-1})].

IR Spectroscopy

An FT-IR absorbance spectrum of a single crystal of $Tm_5(BO_3)_2F_9$ was recorded with transmitted,

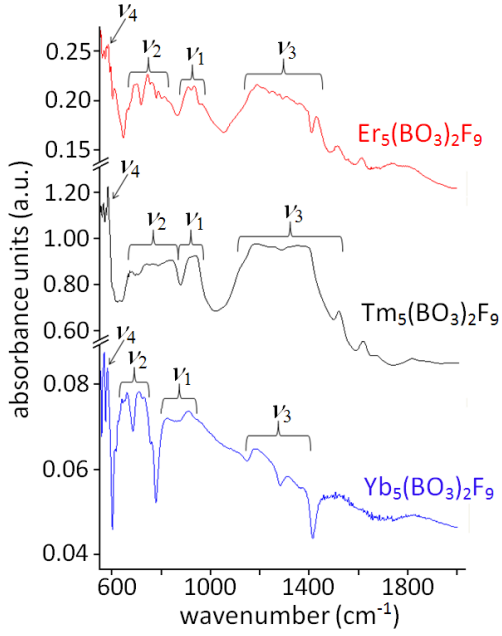

Fig. 3 (color online). FT-IR absorbance spectra of single crystals of $Tm_5(BO_3)_2F_9$, $Er_5(BO_3)_2F_9$, and $Yb_5(BO_3)_2F_9$ in the range of 550 – 2000 cm^{-1}.

polarized light on a BaF_2 plate, using a Bruker Vertex 70 spectrometer, attached to a Hyperion 3000 microscope, a MIR light source, and an LN-MCT detector. The spectral resolution was ∼4 cm^{-1}. The minimum-maximum normalization was realized by the OPUS 6.5 software (Bruker). In Fig. 3, the spectrum of $Tm_5(BO_3)_2F_9$ is compared to the spectra of $RE_5(BO_3)_2F_9$ (*RE* = Er, Yb). The absorption pattern of $Tm_5(BO_3)_2F_9$ resembles those of the isotypic compounds, showing the characteristic absorbances for triangular BO_3 groups [5, 29, 30]. Below 650 cm^{-1}, bands are caused by the in-plane bending (ν_4) of the BO_3 groups. The strong absorptions, induced from the out-of-plane bending (ν_2) of the trigonal group, appear as sharp bands in the range of 650 – 850 cm^{-1}. Due to the crystalline environment, the absorption bands between 900 – 1000 cm^{-1} can be assigned as symmetric stretching vibrations (ν_1). The area of 1150 – 1500 cm^{-1} shows the asymmetric stretching vibrations (ν_3) of the BO_3 groups. The already known single-crystal absorbance spectra of the isotypic phases show two bands in the region of 3400 – 3600 cm^{-1} (Fig. 4), which indicate hydroxyl groups. In the corresponding spectrum of the dried bulk material of the isotypic compound $Yb_5(BO_3)_2F_9$ [5], these bands were not present. The single crystals of all isotypic phases used for IR spectroscopy were exposed to the influence of air and humidity. In consequence, $Tm_5(BO_3)_2F_9$ shows a weak absorption pattern, which may be due to the substitution of fluoride by hydroxyl groups. This is a well known exchange, which apparently differs for the various fluoride borates [4, 5], corresponding to the hygroscopic properties. In apatites, the exchange of hydroxyl and fluoride ions was observed and studied in detail [31, 32].

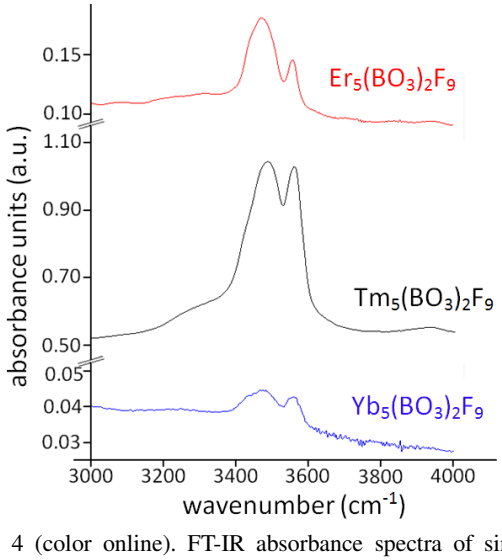

Fig. 4 (color online). FT-IR absorbance spectra of single crystals of $Er_5(BO_3)_2F_9$ (top), $Tm_5(BO_3)_2F_9$ (middle), and $Yb_5(BO_3)_2F_9$ (bottom) in the range of 3000 – 4000 cm^{-1}.

Raman spectroscopy

In the range 100 – 1600 cm^{-1}, a Raman spectrum of a single crystal of $Tm_5(BO_3)_2F_9$ was measured without polarizers, using a Horiba LabRam HR-800 confocal micro-spectrometer and a 785 nm diode laser. The scattered light was dispersed by a grating with 1800 lines mm^{-1} and collected by a 1024 × 256 open electrode CCD detector. The laser focus and the power on the sample surface were ∼1 μm and ∼10 mW, respectively. The depth resolution was ∼4 μm and the spectral resolution ∼2 cm^{-1}. The wavenumber accuracy of ∼1 cm^{-1} was accomplished by regularly adjusting the zero-order position of the grating and checked by a neon calibration lamp. The third-order polynomial background subtraction, normalization, and band fitting by Gauss-Lorentz functions were done by the LABSPEC 5 software (Horiba).

The Raman spectra of the isotypic compounds $RE_5(BO_3)_2F_9$ (*RE* = Er, Tm, Yb) resemble each other

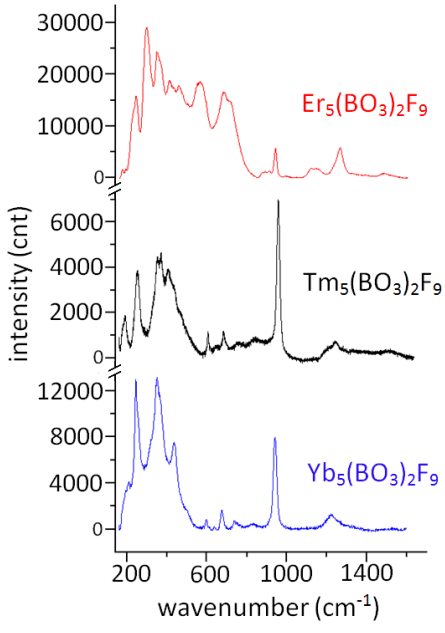

Fig. 5 (color online). Raman spectra of single crystals of $Er_5(BO_3)_2F_9$ (top), $Tm_5(BO_3)_2F_9$ (middle), and $Yb_5(BO_3)_2F_9$ (bottom) in the range of 150 – 1600 cm^{-1}.

(Fig. 5). The most intense bands < 500 cm^{-1} and the narrow, "isolated" band at $\sim$940 cm^{-1} occur in each spectrum. Above 1000 cm^{-1}, one broad band is noticed in the spectrum of $Tm_5(BO_3)_2F_9$. Bands around 900 cm^{-1} in borates are usually caused by stretching modes of BO_4 tetrahedra, whereas those of BO_3 groups are anticipated > 1100 cm^{-1} [4, 33 – 38]. However, in hydrated monoborates, very intense bands were observed at 882 and 501 cm^{-1} and assigned to symmetric stretching vibrations of the isolated BO_3 groups [35]. The unexpectedly high variation of B–O bond lengths inside the BO_3 groups (see above) might be the reason for the comparatively low wavenumber and the large wavenumber range of these bands. Bands < 500 cm^{-1} are evoked by the *RE*–O / *RE*–F bond bending and stretching, as well as lattice vibrations.

Conclusion

With the synthesis of $Tm_5(BO_3)_2F_9$, the missing isotypic compound in the series $RE_5(BO_3)_2F_9$ (*RE* = Er, Tm, Yb) was found and characterized. To investigate the stability field of this structure type, additional experiments in the pressure range 3 – 7 GPa were performed with the neighboring, larger rare-earth cations Ho^{3+}, Dy^{3+}, and Tb^{3+}. Up to now, only structure types similar to that of the compounds $RE_3(BO_3)_2F_3$ (*RE* = Sm, Eu, Gd) [1, 2] and $Gd_2(BO_3)F_3$ [3] were identified.

Acknowledgement

We would like to thank Dr. G. Heymann for collecting the single-crystal data.

[1] G. Corbel, R. Retoux, M. Leblanc, *J. Solid State Chem.* **1998**, *139*, 52.
[2] E. Antic-Fidancev, G. Corbel, N. Mercier, M. Leblanc, *J. Solid State Chem.* **2002**, *153*, 270.
[3] H. Müller-Bunz, Th. Schleid, *Z. Anorg. Allg. Chem.* **2002**, *628*, 2750.
[4] A. Haberer, R. Kaindl, J. Konzett, R. Glaum, H. Huppertz, *Z. Anorg. Allg. Chem.* **2010**, *636*, 1326.
[5] A. Haberer, H. Huppertz, *J. Solid State Chem.* **2009**, *182*, 888.
[6] A. Haberer, R. Kaindl, O. Oeckler, H. Huppertz, *J. Solid State Chem.* **2010**, *183*, doi: 10.1016/j.jssc.2010.06.019.
[7] A. Haberer, R. Kaindl, H. Huppertz, *J. Solid State Chem.* **2010**, *183*, 471.
[8] A. Haberer, R. Kaindl, H. Huppertz, *Solid State Sci.* **2010**, *12*, 515.
[9] K. Kazmierczak, H. Höppe, *Eur. J. Inorg. Chem.* **2010**, 2678.
[10] H. Huppertz, *Z. Kristallogr.* **2004**, *219*, 330.
[11] D. Walker, M. A. Carpenter, C. M. Hitch, *Am. Mineral.* **1990**, *75*, 1020.
[12] D. Walker, *Am. Mineral.* **1991**, *76*, 1092.
[13] D. C. Rubie, *Phase Transitions* **1999**, *68*, 431.
[14] N. Kawai, S. Endo, *Rev. Sci. Instrum.* **1970**, *8*, 1178.
[15] Z. Otwinowski, W. Minor in *Methods in Enzymology*, Vol. 276, *Macromolecular Crystallography*, Part A (Eds.: C. W. Carter Jr., R. M. Sweet), Academic Press, New York, **1997**, pp. 307.
[16] G. M. Sheldrick, SHELXL-97, Program for the Refinement of Crystal Structures, University of Göttingen, Göttingen (Germany) **1997**.
[17] G. M. Sheldrick, *Acta Crystallogr.* **2008**, *A64*, 112.
[18] R. D. Shannon, *Acta Crystallogr.* **1976**, *A32*, 751.
[19] A. S. Wills, VALIST (version 4.0.0), University College London, London (UK) **1998 – 2008**. Program available from www.ccp14.ac.uk.
[20] I. D. Brown, D. Altermatt, *Acta Crystallogr.* **1985**, *B41*, 244.
[21] N. E. Brese, M. O'Keeffe, *Acta Crystallogr.* **1991**, *B47*, 192.
[22] R. Hoppe, S. Voigt, H. Glaum, J. Kissel, H. P. Müller, K. J. Bernet, *J. Less-Common Met.* **1989**, *156*, 105.
[23] R. Hoppe, *Angew. Chem.* **1966**, *78*, 52; *Angew. Chem., Int. Ed. Engl.* **1966**, *5*, 96.
[24] R. Hoppe, *Angew. Chem.* **1970**, *82*, 7; *Angew. Chem., Int. Ed. Engl.* **1970**, *9*, 25.
[25] R. Hübenthal, MAPLE (version 4.0), Program for the Calculation of Distances, Angles, Effective Coordination Numbers, Coordination Spheres, and Lattice Energies, University of Gießen, Gießen (Germany) **1993**.
[26] W. H. Zachariasen, *Skr. Nor. Vidensk.-Akad.* **1928**, 4.
[27] S. V. Berger, *Acta Crystallogr.* **1952**, *5*, 389.
[28] A. Zalkin, D. H. Templeton, *J. Am. Chem. Soc.* **1953**, *75*, 2453.
[29] J. P. Laperches, P. Tarte, *Spectrochim. Acta* **1966**, *22*, 1201.
[30] G. Heymann, K. Beyer, H. Huppertz, *Z. Naturforsch.* **2004**, *59b*, 1200.
[31] V. P. Orlovskii, S. P. Ionov, T. V. Belyaevskaya, S. M. Barinov, *Inorg. Mater.* **2002**, *38*, 182.
[32] A. Knappwost, *Naturwissenschaften* **1959**, *46*, 555.
[33] H. Emme, H. Huppertz, *Chem. Eur. J.* **2003**, *9*, 3623.
[34] H. Huppertz, *J. Solid State Chem.* **2004**, *177*, 3700.
[35] L. Jun, X. Shuping, G. Shiyang, *Spectrochim. Acta* **1995**, *A51*, 519.
[36] G. Chadeyron, M. El-Ghozzi, R. Mahiou, A. Arbus, J. C. Cousseins, *J. Solid State Chem.* **1997**, *128*, 261.
[37] J. C. Zhang, Y. H. Wang, X. Guo, *J. Lumin.* **2007**, *122 – 123*, 980.
[38] G. Padmaja, P. Kistaiah, *J. Phys. Chem.* **2009**, *A113*, 2397.